EUROPEAN ORGANIZATION FOR NUCLEAR RESEARCH

M. G. DOME III

CERN-ISR-VA/82-18

Closed distribution

X-RAY INDUCED GAS DESORPTION WITHIN A PROTOTYPE LEP VACUUM CHAMBER

by

E.M. Williams*, F. Le Normand, N. Hilleret and G. Dominichini

Geneva, December 1982

* Visitor from the University of Liverpool,
Department of Electrical Engineering and Electronics

Introduction

The important role of surface processes in the attainment of ultra-high vacuum in storage rings for high-energy particles is exemplified by developments at the I.S.R. over the last few years (Calder 1974, Fischer 1977). This background of work is most relevant in approaching the design of the new LEP accelerator, yet the surface processes leading to the deterioration of vacuum with electron machines are quite distinct from those applicable to proton storage rings. With proton machines the perturbing action is identified with ion bombardment of surfaces leading to the desorption of surface gas in a manner which follows, in general terms, the model of a binary collision involving momentum transfer to an adatom (Heiland and Taglauer 1978, Hilleret 1980). In contrast, the problems at electron machines emanate from the intense synchrotron radiation, with the probable gas desorption process involving the participation of photoelectrons in electronic excitation of the adsorbate (Fischer and Mack 1965, Redhead et al 1968). For the more energetic photoelectrons generated by the radiation the process of energy loss conforms with the notion of a diffusion phenomenon into the bulk, and in consequence in this case subsurface gas may be activated to the surface to be desorbed (Garwin et al 1968). The difference in operation between proton and electron machines is immediately seen with beam induced cleaning which can occur to an appreciable degree with electron storage rings (Thompson 1975, Trickett 1978). In this situation it is by no means possible to extrapolate to electron machines those procedures and treatments which have been successfully applied to proton storage rings.

The present report is concerned with an experimental simulation of the process of photon induced desorption within an aluminium vacuum chamber of the same basic form as proposed for the LEP accelerator. Investigations have been made using a commercial X-ray source and were foreseen as complementary to investigations concurrently underway at Orsay using synchrotron light from the 1.72 GeV electron storage ring (Gröbner et al 1981) and measurements on NEG pumped vacuum chambers installed on the 17 GeV electron storage ring (PETRA) at DESY, Hamburg (Benvenuti, 1982). The objectives in the work can be described in the following three-fold manner : Firstly, to establish the levels of photon induced desorption efficiency for identified gas species.

Secondly, to examine the contribution of surface treatments as bakeout and glow discharge cleaning, and to correlate these responses with changes in surface activity induced by beam cleaning. Thirdly, to gain insight into the energy dependence of the desorption process so as to provide a reasonable basis for predicting conditions at the levels of critical energy* in excess of 100 keV which are applicable at the full design energy of the LEP accelerator. This latter objective is of particular note in regard to tests using an X-ray generator, since an X-ray source offers the possibility of extending measurements to higher levels of photon energy than are available with storage rings, as at Orsay, operating at a peak electron energy of a few GeV. In relation to the role of photon energy, it is of interest to note that at photon energy above ~ 50keV the cross section for Compton interaction exceeds that of photoelectron generation - a maximum in the photoelectron cross section occurs at the K-edge of aluminium at 1.6 keV (Evans 1958).

The levels of desorption efficiency for vacuum stability in the LEP machine, based on reasonable assumptions of pumping speed and beam lifetime should be below 10^{-5} molecule photon^{-1}, at least for the heavier gas molecules as CO and CO_2 (LEP, 1979).

Experimental system and procedure

The basis of the study is the observation of the pressure pulse of desorbed gas accompanying the introduction, in step fashion, of a photon flux to the interior of the vacuum system. The equipment utilised in the tests is shown schematically in Fig. 1. The sample of aluminium chamber, of Extrudal alloy (Al-MgSi 0.5), was cut form a length of prototype tube manufactured for the LEP project. One end of the metre long sample was coupled to a stainless steel chamber housing the X-ray tube, while the other end was connected to

---

* The critical energy characterises the spectral power distribution of the synchroton radiation; it is the energy setting around which the radiative power is equally distributed.

a further stainless steel chamber housing the diagnostic instruments. These comprised a total pressure gauge and a quadrupole mass spectrometer, model Balzers 112. The diagnostic chamber, in turn, was connected via an orifice of conductance 40 $l\,s^{-1}$ for N_2 to a 400 $l\,s^{-1}$ ion pump and a sublimation pump providing an active area of around 1500 cm^2. The sample along with other components of the vacuum system was cleaned following the stages of liquid and vapour phase treatments forming the basis of the standard ISR cleaning procedure (Erlandsson 1980).

The X-ray unit was a Philips model PW 2181/00 fitted with a gold target and with the sealed tube head incorporating a 1 mm thick beryllium window. Accelerating voltages variable in the range up to 100 kV were derived from a stabilised d.c. voltage supply with maximum output power of 3 kW. Vacuum isolation between the stainless steel chamber housing the X-ray head and the aluminium vacuum chamber under test was provided by a membrane formed of aluminium foil 25 μm thick. Initial attempts were made to provide vacuum isolation using a sheet of Kapton thickness 75 μm, but as will be mentioned later in the text problems were encountered with this material under the particular conditions of the tests. Under typical operating conditions the pressure in the source chamber, pumped by a turbomolecular pump, was held at a few times 10^{-6} torr with ultra-high vacuum in the main test chamber. The radiation from the source was within $\pm$ 13° of the central ray which was aligned with the longitudinal axis of the aluminium chamber. In this manner, direct irradiation of the aluminium test chamber commenced some 14 cm beyond the end of flange near the aluminium window, with altogether some 3,500 cm^2 of the test chamber under irradiation together with a further 200 cm^2 of the diagnostic chamber. The radiation could be interrupted from the chamber by means of of a moveable lead shutter incorporated into the source chamber and which could be operated remotely.

The desorption efficiency expressed as M_γ the number of desorbed molecules per incident photon follows most conveniently from observations of the change in the equilibrium levels of total and partial pressures accompanying irradiation. In terms of the change in total gas pressure Δp, a total desorption

efficiency expressed in N_2 equivalent pressure follows as :

$$M_{\gamma}(N_2) = \frac{\Delta p\ (N_2 \text{ equivalent}) \times S \times a}{\text{no. of photons arriving per second}} \quad . \qquad (1)$$

Here a is a constant to convert torr l to number of molecules and S the pumping speed, i.e. the conductance of the pumping orifice for N_2. The number of photons relates, of course, to the total number of photons contained within the spectral output of the X-ray generator; as such, the desorption efficiency relates to a range of photon energies.

The greater interest with the determination of desorption efficiency lies with the identification of desorption efficiency appropriate to each species of desorbed gas. This is given in terms of the change accompanying irradiation of the current of species j at the quadrupole, $\Delta i(j)$, as:

$$M_{\gamma}(j) = \frac{\Delta i(j) \times S(j) \times a}{C_q(j) \times t \times i_e \times \text{no. of photons arriving per second}} \quad , \qquad (2)$$

where $C_q(j)$, t and i_e are respectively the relative sensitivity factor, the general transmission term and the emission current at the quadrupole formulated by writing the change in ion current in terms of the change in partial pressure as:

$$\Delta i(j) = \Delta p(j) \times t \times C_q(j) \times i_e \quad . \qquad (3)$$

The relative sensitivity factor could be measured under the conditions of the experiment by injecting the gases of interest and calibrating the response in terms of the known sensitivity of the total pressure guage. These relative sensitivity factors can be expected to remain constant in time, but the absolute sensitivity will change as with ageing of the electron multiplier at the quadrupole etc. To compensate for this, the general transmission term was found for each measurement using the observed change in total pressure according to:

$$\Delta p = \frac{1}{K \times t \times i_e} \sum_j \Delta i(j) \frac{C_t(j)}{C_q(j)} \quad . \qquad (4)$$

K is a constant factor defined for the particular total pressure measuring system by the ratio of the indicated pressure to the ion current at the gauge. $C_t(j)$ is the sensitivity of the total pressure gauge for species j. The result (4) is based on the superposition of partial pressures.

To proceed with the evaluation and the characterisation in energy of the desorption efficiency M_γ then, of course, the photon flux as well as its energy distribution must be known. In principle, various theoretical approaches based on Kramer's theory (1923) of bremsstrahlung energy emission can be applied (Dyson 1973, Unsworth and Greening 1970, Birch and Marshall 1979a) but there always remains uncertainty as to the contribution of characteristic line emission as well as factors such as electron backscattering which causes the spectrum to be deficient in low energy photons. Measurements of the X-ray spectra from thick gold targets under the conditions employed here have not been located in the published literature. For these reasons an experimental determination of the photon spectrum was embarked upon in our work, making use of a solid-state detector formed of germanium of ultra-high purity (Ewan 1979) in conjunction with standard techniques of pulse height analysis. The operation of the detector, Schlumberger model EGPP 100S, was investigated using a series of calibrated radionuclei sources emitting X-rays from internal conversion or electron capture (Campbell and McNelles 1975). The findings in this preliminary work verified the constant sensitivity for photon detection over the energy range 5-90 keV and also confirmed the linearity of the photon energy scale. In application with the X-ray source, the problem was the correct attenuation of the photon flux to a level compatible with a counting rate below 50 $k\,s^{-1}$ in order to avoid coincidence effects which distort the photon distribution in favour of high energy photons (Storm, Israel and Lier 1968). The procedure followed was to restrict the sampling area with an aperture approximately 0.2 mm diameter in a 1 cm thick lead plate placed in front of the detector, while operating with minimum current in the X-ray tube (3.2 mA) and with the source to detector distance at the maximum value of 1.4 m which could be accommodated in the experimental enclosure. Examples of photon energy spectra

determined in this way and allowing for air absorption, which largely influences photons at energies below ~11 keV, are given in Fig. 2 for tube voltages of 20, 40 and 80 kV. Here the ordinate scale presents the number of photons n per 100 eV bandwidth plotted in arbitrary units. The characteristic emission lines of the gold L-series at energies 9.7, $11.5 \pm .1$ and 13.3 keV are quite distinct in all cases (the K-edge of gold at 80.7 keV lies higher than the energy limit investigated). These characteristic lines are seen to be superimposed on the continuum radiation which in the case of each spectrum extends to an upper limit identified with the tube voltage; on the low energy side the cut off below 7 keV is entirely compatible with the filtering imposed by the beryllium and aluminium windows of the source arrangement.

In these measurements the relative sensitivity of photon dectection was known, however, in view of the lack of geometric precision of the arrangement for attenuating the photon flux it is not possible to fix the absolute scale of the number of photons with any real confidence. An alternative approach in this goal is to fix the efficiency of conversion from electrical to radiant power using the calibration of X-ray generators performed by workers in other laboratories. Following the pioneering work of Compton and Allison (1935) the efficiency of X-ray production ε is written as :

$$\varepsilon = \frac{\text{X-ray power}}{\text{Cathode-ray power}} = k \times V \times Z \quad , \qquad (5)$$

where Z is the atomic number of the target material, V the tube voltage and k a constant of proportionality in units of reciprocal volts. The determination of the constant k and its possible dependence on Z and V has been the subject of research over many years (see Evans 1955, Dyson 1973), but in more recent times the topic has been pursued by workers at the Cavendish and the Los Alamos Laboratories (Dyson 1973, Storm, Israel and Lier 1968, Storm and Lier 1972). These more recent studies taken with the findings of earlier research point to the generalisation of the setting of k as $(0.6 \pm 0.4) \times 10^{-6}/4\pi$ $kV^{-1}\,sr^{-1}$, but with indications of a variation in k due to Z and V individually. The results of

the present observations of spectra treated to yield relative values of k as a function of tube voltage are shown in Fig. 3. The values were derived by forming $\sum n(E)\,E$ over each of the measured spectra while taking into account factors as the data collection time and the tube settings. The increase in k with rising tube voltage is quite apparent; this can be understood in part at least as due to the influence of the windows since inevitably below around 7 kV the efficiency must fall to zero. However, following the experience of Storm et al at Los Alamos the type of voltage supply used for exciting X-ray spectra should also be borne in consideration. They found that with spectra derived from stabilised d.c. supplies providing constant output voltage (as employed in the present study) there is a tendency for k to increase with increasing voltage. In quantitative terms the extent of the increase for a 60 kV X-ray unit with a tungsten anode was by a factor of two over the range 10-60 kV, this compares with a factor of 3 in the data of Fig. 3 for the voltage range 20-80 kV.

The form of the data depicted in Fig. 3 points to an asymptotic limit to k at high voltage, in keeping with the trends in the work of Storm et al. On this basis the value of k obtained by projecting the data of Fig. 3 to a voltage of 120 kV is taken as the generalised value $0.6/4\pi \times 10^{-6}\,kv^{-1}\,sr^{-1}$ already noted in the text, thus fixing an absolute scale of k. With the exit aperture of the X-ray head of $\pm 13^{o}$ the effective efficiency of the source is correspondingly 0.0003% at 20kV and increases to 0.004% at 80 kV. The total number of photons emitted per second from the X-ray head (i.e. within $\pm 13^{o}$), based on this calibration, is shown in Fig. 4 plotted as number per second against tube voltage with the tube current at 8 mA - observations of the output from the X-ray generator as a function of tube current are consistent with a proportionality between output and tube current (as will be discussed shortly). Also included in Fig. 4. is the mean energy of the radiation, found by numerical analysis of the spectra, which can be seen to range from 9.5 keV at 15 kV tube setting to 31 keV at 80 kV setting. It is of interest to note that the total number of photons emitted per second found in this way is greater by a

factor 5.8 than the total number found by considering the geometry of the arrangement for attenuating the photon flux, i.e. treating the sampling aperture as precisely 0.2 mm diameter. Following both approaches there is the assumption of an uniform distribution of photon flux over the exit aperture of $\pm$ 13°, however, this assumption would appear to be quite reasonable (Meredith and Massey, 1968, Dyson, 1982). Published values by Brumbach and Kaminsky (1976) for the total photon flux of a General Electric 50 keV X-ray unit fitted with a tungsten anode are within a factor 2 of the data of Fig. 4. Similarly, data contained in the Catalogue of Spectral Data for Diagnostic X-rays published by AERE, Harwell (Birch and Marshall 1979 b), are consistent with the present findings of photon flux output to within a factor of 2. The accuracy of the scale of total output flux depicted in Fig. 4 is estimated as within a factor of 2.

Results

Preliminary observations and the role of parameters of the source

The first attempts at measurements of desorption efficiency were carried out using a Kapton window 75 μm thick to isolate the source chamber. The experience as evolved in the course of these preliminary investigations pointed to the non-suitability of Kapton in this application where it was not possible to bake and to attain u.h.v. conditions at each side of the window membrane - in contrast to a particular situation in the I.S.R. where Kapton is successfully exploited. In all cases after bakeout of the aluminium chamber at 150° C, the signal of H_2O with, typically, a base pressure of 3 x 10^{-10} torr amounted to at least 50% of the major peak identified with hydrogen. Moreover, long term irradiation of the chamber led to further significant evolution of water and to the destruction of the quality of vacuum - the situation could then be remedied only with a further bakeout.

The more satisfactory response was obtained with the establishment of an aluminium window formed with material 25 μm thick. With bakeout at 150° C the residual pressure improved to 5 x 10^{-11} torr, typically, with the gas spectrum reflecting the clear dominance of hydrogen. The minor gas species discernable above the noise were CO and CO_2 with, respectively, peak heights around 7% and 4%

of the hydrogen peak. With irradiation of the baked system under conditions 15 kV, 8 mA at the X-ray source, chosen to minimise the level of excitation, the total desorption efficiency was found close to 10^{-1} mol photon^{-1}. The partial desorption efficiencies in order of preponderance were identified as CO_2, H_2, CO, CH_4, the first two gases constituting in excess of 80% of the total activity. Examples of records of the total and the partial pressures accompanying irradiation are provided in Fig. 5. The recordings are arranged to coincide at the point of opening the shutter at t=0, but the duration of the exposure is not uniform; the instant of termination is indicated by an arrow in each case. The speed of response with the introduction and cessation of the radiation is of the order 5s, largely governed by the electronic time constant of the current measuring equipment. There is a tendency for the background level to change slowly in the course of irradiation. This is exemplified in Fig. 5. by the finite slope at the flat-top of the total pressure pulse, also the recovery to the original base level upon termination can be seen to be somewhat delayed. Modifications of this kind to the ideal pulse response have previously been reported particularly in researches at Brookhaven National Laboratory (Edwards et al 1977, Edwards 1978) and can be regarded as an enhancement of outgassing rate induced by bombardment. To a first approximation the findings in our work indicated a proportionality of the effect with the magnitude of the photon flux whether increased by increasing current or voltage at the X-ray source. In the evaluation of desorption parameters this influence could be accounted for identifying the change in base level, and this gave a correction at most around 10% to the apparent pressure change.

The behaviour of the pressure pulses with variation in current at the X-ray tube is illustrated in Fig. 6. which shows data for CO_2 pulse height over the current range 5-40 mA and for two fixed values of tube voltage. The proportionality which is evident was a feature of all gas species and of the total pressure pulse as a function of current. These findings are in keeping with a proportionality between the number of photons and the tube current together with the identification of a first-order process of desorption. The dependence of the desorption pulse height on voltage at the X-ray tube with constant tube current

is illustrated in Fig. 7. which contains the results of measurements with hydrogen partial pressure and with total gas pressure. Over the range of measurement the response is linear with a cut-off in the region of 8 kV, just at the threshold voltage for photon transmission. This form of result was consistently deduced at all stages in the work for all gas species and following different pre-treatments at the chamber. When reconciled with the variation in photon number with tube voltage (Fig. 4), the linear form of the pressure pulse height with voltage leads to the conclusion that the desorption efficiency decreases with increasing photon energy.

Desorption efficiencies with pretreatments and with extensive bombardment

Under the conditions of the tests so far described, care was taken to minimise the exposure of the chamber to radiation thereby offsetting the possibility of any beam-induced change. On the other hand the influence of continual intense bombardment and its perspective with treatments of bakeout and glow discharge cleaning formed an essential objective of the programme of work. In the event the effect of continual photon irradiation under the conditions of the experiment proved to be low, as will be discussed below. In presenting the findings of the work it is convenient first to examine the role of bakeout and of glow discharge treatment with the photon flux serving as a tool to sample the desorption activity at the surface. The normal approach in sampling was to employ conditions 15 kV, 8 mA at the X-ray source, thereby introducing a total sampling flux of 1.4×10^{11} photons s^{-1} at a mean energy of 9.5 keV.

The values of desorption efficiency following different pretreatments are given in Table I which contains data with unbaked, baked, and glow discharged systems. Glow discharge treatment with argon gas was carried out in the standard I.S.R. manner with a wire anode placed along the axis of the aluminium chamber and its associated diagnostic chamber. The discharge was operated at a temperature of 150°C and provided an estimated ion dose of 5×10^{18} ions cm^{-2}. Subsequently the system was filled with nitrogen for re-assembly with the X-ray facility. Thereafter, measurements of desorption efficiency were carried out

Table 1 Desorption Efficiencies with Different Pre-Treatments

Measured with a flux of 1.4×10^{11} photons s^{-1} at mean energy 9.5 keV over an irradiated area $\sim 4 \times 10^{3}$ cm^{2}

Chamber non-treated by glow discharge	System Pressure (torr)	M_γ (total) N_2-equiv. (mol. photon^{-1})	Partial Desorption Efficiency (mol. photon-1)				M_γ (total) (mol. photon^{-1})
			H_2	CO_2	CO	CH_4	
Unbaked	1.5×10^{-8}	4.5×10^{-1}	2.4×10^{-1} (44%)	2.6×10^{-1} (48%)	3.2×10^{-2} (6%)	1.4×10^{-2} (3%)	5.5×10^{-1}
Baked	6×10^{-11}	1×10^{-1}	2.5×10^{-2} (29%)	5.5×10^{-2} (63%)	5×10^{-3} (6%)	2×10^{-3} (2%)	8.7×10^{-2}
Chamber glow discharge treated							
Refitted and unbaked	1.5×10^{-8}	1.5×10^{-1}	2.3×10^{-1} (76%)	$5. \times 10^{-2}$ (17%)	1.5×10^{-2} (5%)	8×10^{-3} (3%)	3.0×10^{-1}
Baked	6×10^{-11}	7×10^{-2}	6×10^{-2} (61%)	2.6×10^{-2} (26%)	8×10^{-3} (8%)	5×10^{-3} (5%)	1×10^{-1}
Exposed to air and re-evacuated	5×10^{-9}	1.5×10^{-1}	1.3×10^{-1} (60%)	7.5×10^{-2} (34%)	1×10^{-2} (5%)	2×10^{-3} (1%)	2.2×10^{-1}
Further Bakeout	5×10^{-11}	6.5×10^{-2}	3.8×10^{-2} (47%)	2.8×10^{-4} (35%)	1.2×10^{-2} (15%)	3×10^{-3} (4%)	8.1×10^{-2}

sequentially following the stages of i) evacuation at room temperature only, ii) bakeout at 150°C, iii) exposure to air for 24h followed by evacuation at room temperature, and, finally, iv) bakeout at 150°C. In all cases the bakeout period was 24 h. The table contains values of the total desorption efficiency formed according to the change in nitrogen equivalent readings of pressure (column 3) as well as the correct total desorption efficiency formed by summing the individual, partial values of desorption efficiency (column 8). It is of interest to note that these are at least within a factor or two of each other. The partial desorption efficiencies are identified with H_2, CO_2, CO and CH_4 in all cases of pretreatment; the figures in parenthesis identify the percentage contribution of each species to the total desorption efficiency. A feature of particular note is the absence of an argon desorption signal following discharge treatment. The argon signal in the residual gas was not discernible above the noise (signal to noise for hydrogen would be typically 100:1) and no enhancement was seen with irradiation - even with an augmentation of the photon flux well beyond the normal sampling value. An upper limit for argon desorption can be placed at 5×10^{-5} mol. photon^{-1}. The values of total desorption efficiency (column 8) amongst the various pretreatments range from 8×10^{-2} to 5×10^{-1} mol. photon^{-1}, clearly a rather narrow distribution of values. There is a group of total desorption efficiencies at 5.5×10^{-1}, 3×10^{-1} and 2.2×10^{-1} mol. photon^{-1} associated with chambers in an unbaked condition, and a further block at the lower values of 8.7×10^{-2}, 1×10^{-1} and 8.1×10^{-2} identified with baked chambers - on the basis of this grouping the contribution of glow discharge cleaning is indistinct. For the partial desorption efficiencies it can be seen from the table that the dominant species in all cases are H_2 and CO_2 which contribute at least 80% to the total desorption activity. There is, however, a diminution in the relative contribution of CO_2 following glow discharge treatment. In the absence of glow discharge treatment the desorption of CO_2 is largest, although only marginally when unbaked, whereas with the inclusion of the treatment H_2 is the greatest. In absolute terms the decrease in CO_2 is by around 50% for the case of a bakeout prior to each

measurement. A justification for the inclusion of glow discharge treatment, based on this level of change, is clearly questionable.

The results of studies designed to reveal the effect of any photon-induced change in the surface response are illustrated in Figs. 8a and 8b which show the evolution of desorption efficiency (total, N_2 equivalent, and partial) on a daily basis while operations of intense photon bombardment were pursued. The photon dose (i.e. the product of the output photon flux per second and the irradiation time) at various stages in the investigation are indicated in the diagram, while the corresponding settings of the X-ray source are listed in the figure caption. Fig. 8a refers to measurements to a cumulative, overall dose of 7×10^{17} photons obtained with a baked chamber which while having been glow discharge cleaned in its early history, had also served in many of the preliminary tests. The measurements of Fig. 8b were obtained following a further cycle of glow discharge cleaning of the same test chamber and after further bakeout in the test facility. It can be seen from the figures that the diminution of desorption signal with treatment is a weak effect - at most there is a 25% reduction for CO_2 and CO over the whole programme of treatment depicted in Fig. 8a The precision of measurement over long term can at best be claimed at $\pm$ 10% thus there is some difficulty in claiming the effect as real.

An indication of the continual, high level of gas production under bombardment had emerged in the course of preliminary tests, and it had been seen that the build-up of CO_2 in the course of intensive bombardment had a detrimental effect on the recovery of ultra-high vacuum. For this reason the bombardments depicted in Fig. 8 were operated in cycles of one minute duration followed by an off period of four minutes in order to allow for the removal of gas - in this way the system pressure was always kept below 2×10^{-9} torr. Most sampling measurements were carried out some ten hours after the termination of each bombardment stage with the system pressure restored to a level below 10^{-10} torr. However, in a few cases, for which the corresponding data points are enclosed by dashed lines, measurements were made as soon as practicable at the end of bombardment with the system pressure at $\sim 2 \times 10^{-10}$ torr. These

measurements indicate neither an augmentation nor a reduction in desorption efficiency relative to the more customary sampling procedure, which points to the insensitivity of the surface condition to the ambient atmosphere. This reinforces the view of a stable surface condition with negligible change induced by irradiation over long term. In quantitative terms, noting values of a total flux of some 7×10^{17} photons over an area of 3.5×10^{3} cm^2 and with a desorption efficiency of 10^{-1} mol. $photon^{-1}$, the scale of total gas removal is around 2×10^{13} mol. cm^{-2}; the conclusion to be drawn is that the level of gas accommodation leading to desorption at the continual high level is at least close to one monolayer.

Discussion and Conclusions

The identification of hydrogen, carbon dioxide, carbon monoxide and methane as the desorbed species under irradiation with X-rays follows the pattern established in earlier work with electron and ion bombardment both with aluminium and other technological metals (Achard 1976, Achard et al 1979, Erlandsson 1980, Vaughan-Watkins and Williams 1980). The only previous simulation of X-ray bombardment that we are aware of in the published literature is due to Brumbach and Kaminsky (1976) who investigated the desorption at aluminium and stainless steel surfaces using a commercial X-ray unit providing photons in the range 10-50 keV. In their work a signal of molecular oxygen in addition to the dominant carbon dioxide desorption was observed; this conflicts with the present findings and the findings, in general, with stimulii of electrons and ions at technological surfaces. The levels of total desorption efficiency deduced from the measurement of Brumbach and Kaminsky are contained within upper and lower limits of,respectively, 2×10^{-3} and 1×10^{-4} mol. $photon^{-1}$ which is lower than the present findings. The investigations of Brumbach and Kaminsky were carried out with relatively small areas of surface irradiation (~ 8 cm^2) and with a photon flux density at the surface considerably higher in value than that employed in the present study. Some indication of beam induced cleaning was noted in the course of their work, in contrast with the negative response found in the present study.

This difference is likely to be correlated with this role of the photon flux density in defining the extent of beam induced cleaning. It is relevant to note that the total accumulated photon flux over the entire period of the present tests, at around 10^{18} photons, is equal to the total photon flux introduced per metre length of vacuum chamber in the LEP machine with some 15 min of operation (at injection energy and with around 1 mA of circulating beam current). The synchrotron light facility at Orsay provides a more practicable basis for simulating the process of beam induced cleaning in the LEP machine, although with the limitation of a photon spectrum largely devoid of photons at energy above 5 keV. The results recently reported from the experiments with unbaked and baked aluminium chambers carried out at Orsay (Gröbner et al 1981) are of a pattern of gas desorption with H_2, CO_2, CO and CH_4 in accord with the present observations. Moreover, the order of preponderance of the photon desorption effeciencies inferred from measurements with an unbaked chamber taken at the onset of irradiation, is similar; the numerical values of desorption efficiency are to within a factor of 3 of the corresponding data of the present investigation with an unbaked chamber as presented in row 1 of Table I. A strict interpretation of this finding is complicated in view of the energy distributions of the photon flux from the synchrotron source and from the X-ray generator. However, the result certainly stresses the contribution to desorption efficiency of photons at energy around 10 keV, as identified with the mean energy of the photon flux employed with the data presented in Table I.

The role of photon energy in the desorption process, as deduced from the present studies of desorption as a function of voltage at the X-ray tube, is illustrated in Fig. 9, plotted as photon desorption efficiency (arbitrary units) versus tube voltage. The axis of abscissa is identified also in terms of the mean energy of the radiation. The form of result depicted here is characteristic of all gas species and of all stages of vacuum and surface preparation. There is seen a three fold decrease in desorption efficiency as the mean energy increases from 9.5 to 31 keV, with the greatest change occurring over the initial range of mean energy from 9.5 to around 15 keV. A similar pattern of behaviour was

observed in the study of Brumbach and Kaminsky with aluminium samples of small scale. The photon absorption cross-section in aluminium decreases with increasing energy in the X-ray region, although above around 40 keV the rate of fall off is decreased as the contribution of Compton scattering becomes more predominant. The form of the result of Fig. 9 would seem, in general terms, to reflect these features of the total absorption cross-section. It is significant to note that in the high energy limit where the influence of Compton scattering is most active, there is no enhancement in desorption efficiency beyond that observed at lower photon energy.

It is of interest at this stage to examine the energy dependence of the photon desorption efficiency in terms of the production of photoelectrons as a function of energy, in view of the association of gas desorption with electron activity as originally proposed by Fischer and Mack (1965). Following Burke (1977) and Chadsey et al (1975) the photoelectron yield at aluminium surfaces over the range of photon energies employed in the present tests may be written as :

$$\text{yield} = 74.8 \times (\text{Energy eV})^{-1.2} \quad . \qquad (6)$$

Use has been made of this result in conjunction with the measured spectra to evaluate the relative, total number of photoelectrons for a series of settings of voltage at the X-ray tube. (In this task a summation of the product of photon number and yield was carried out over the range of energy contained in each spectrum). When correlated with the measurements of gas desorption as a function of tube voltage it is found that the number of desorbed molecules per photoelectron created by the radiation decreases by only 20% over the range of mean photon energy from 9.5 to 31 keV associated with tube settings of 15 and 80 kV. Direct measurements of electron desorption efficiency at technological surfaces indicate an electron desorption efficiency largely independent of electron energy at above $\sim$1 keV (Achard 1976, Vaughan-Watkins and Williams 1978). The small change in the calculated number of desorbed molecules per photoelectron created by the X-rays identifies a similar trend,and suggests the association of desorption with photoelectron production. The result may, however, be fortuitous in so far that the energy and spatial distribution of the photoelectrons may change with

increasing mean energy of the X-ray output. But on the basis that spatial considerations are not of significance, the association would seem to be possible providing either i) the form of the photoelectron energy distribution is unchanged with increasing mean photon energy, or ii) the number of electrons in the photoelectron spectrum is dominated by electrons of energy above 1 keV. There remains, nevertheless, some concern with the procedure here of extrapolating measurements of photoelectron yield and of electron desorption obtained with small samples to the conditions of large vacuum chambers, in view of the possibility of multiple interactions which would not be applicable with a small target.

The results of the present investigation point to the weak influence of glow discharge cleaning as a surface treatment. There is a displacement of carbon dioxide as the leading desorption signal brought about by the treatment, but the scale of change is rather limited. Hydrogen and carbon dioxide together form consistently the dominant part of the total desorption activity which varies between at most 5×10^{-1} mol. electron^{-1} in the untreated, unbaked state to around 9×10^{-2} mol. electron^{-1} following bakeout. Previously, researches with electron fluxes at technological surfaces have demonstrated the advantages of preparatory glow discharge treatment as adopted here (Jones, Jones and Williams 1973, Vaughan-Watkins and Williams 1978, 1980), as indeed does the whole background of operational experience at the I.S.R. (Calder et al 1977, Fischer 1977). Nevertheless there is conflicting evidence from tests at Desy (Kouptsidis and Mathewson 1976) to suggest that glow discharge treatment at aluminium chambers is only really beneficial when operated in situ. The lack of a clear consensus as to the value of preparatory glow discharge cleaning must somehow reflect differences in experimental conditions. Traditionally, I.S.R. treatments have been carried out at 300° C in contrast to the lower temperature cycle with aluminium chambers during glow discharge cleaning. Further, one may possibly speculate on the difference in response between aluminium and other technological materials found by Achard et al (1979) in their study of ion and electron desorption efficiences as a function of bakeout temperature - thereby identifying a fundamental difference with aluminium. It is interest to note that with in situ glow discharge

cleaning at stainless steel surfaces of small scale Brumbach and Kaminsky found a reduction of around one order of magnitude in the X-ray induced desorption, the only identifiable gas after treatment being carbon dioxide.

In summary, therefore, the values of photon desorption efficiency found in the investigation are significantly higher than those required for stable vacuum operation in the LEP machine. The pretreatment with glow discharge cleaning during bakeout at 150°C is not found to provide a marked advantage beyond the levels of photon desorption efficiency obtained with bakeout alone at 150°C carried out *in situ*. The X-ray equipment is not found to lend itself to a study of beam induced cleaning in vacuum chambers of large scale in view of the relatively low photon flux density over the irradiated surface. On the other hand it has been demonstrated that in the range of photon energies where the contribution of Compton scattering becomes increasingly important, the photon desorption efficiency is not increased beyond the level found at lower energy.

Acknowledgements

The technical support from Mr. L. Derivaz in the course of our tests and the work of Mr. A. Grillot with glow discharge cleaning is gratefully acknowledged. The stimulation of discussions with Drs. R. Calder, O. Gröbner, and H. Störi is very much appreciated. Further, the helpful comments on the script by Dr. R. Calder is gratefully acknowledged.

References

Achard, M.H., 1976, CERN-ISR-VA/76-34.

Achard, M.H., Calder, R. and Mathewson, A., 1979, Vacuum 29, 53.

Benvenuti, C., 1982, Nuclear Instruments and Methods, to be published.

Birch, R. and Marshall, M., 1979a, Phys. Med. Biol., 1979, 24, 505.

Birch, R. and Marshall, M., 1979b, Catalogue of Spectral Data for Diagnostic X-rays, Sci. Report Series No. 30, A.E.R.E., Harwell.

Brumbach, S. and Kaminsky, M., 1976, J. Nuc. Mat. 63, 188; J. App. Phys. 47, 2845; Proc. 6th Symposium on Eng. Prob. of Fusion Research, I.E.E.E. Cat. no. 76 CH1097-5-NPS, p. 1135.

Burke, E.A., 1977, IEEE Trans. Nuc. Sci. NS-24, 2505.

Calder, R.S., 1974, Vacuum 24, 437.

Calder, R., Grillot, A., Le Normand, F.and Mathewson, A., 1977, Proc. 7th Int. Vac. Cong. and 3rd Int. Conf. Sol. Surf., Vienna, Vol. 1, p. 231.

Campbell, J.L. and McNelles, L.A., 1975, Nuc. Inst. Meth. 125, 205.

Chadsey, W.L., Wilson, C.W. and Pine, V.W., 1975, IEEE Trans. Nuc. Sci. NS-22, 2345.

Compton, H.A. and Allison, S.K., 1935, 'X-rays in Theory and Experiment' (Van Nostrand : New York).

Dyson, N.A., 1973, 'X-rays in Atomic and Nuclear Physics' (Longman ; London).

Dyson, N.A., 1982, Private Communication.

Edwards, D., 1978, J. Vac. Sci. Technol. 15, 1586.

Edwards, D., Halama, H. and Aggus, J., 1977, Proc. 7th Int. Cong. and 3rd Int. Conf. Sol. Surf. Vienna, Vol. I, p. 215.

Erlandsson, R., 1980, Appl. Surf. Sci. 6, 473.

Evans, R.D., 1955, 'The Atomic Nucleus' (McGraw Hill).

Evans, R.D., 1958, Handbuch der Physik 34, 218.

Ewan, G.T., 1979, Nuc. Inst. Meth. 162, 75.

Fischer, E., 1977, IEEE Trans. Nuc. Sci. 24, 1227.

Fischer, G.E. and Mack, R.A., 1965, J. Vac Sci. Technol. 2, 123.

Garwin, E.L., Hayt, E.W., Rabinowitz, M. and Jurow, J., 1968, Proc. 4th Int. Vac. Congress, Manchester, p. 131.

Gröbner, O., Mathewson, A.G., Störi, H., Strubin, P. and Souchet, R., 1981, CERN-ISR-VA/81-31.

Heiland, W. and Taglauer, E., 1978, Inst. Phys. Conf. Ser. No. 38, p. 287.

Hilleret, N., 1980, Proc. 4th Int. Conf. Sol. Surf and 3rd European Conf. Surf. Sci., Cannes, Vol. II, p. 1221.

Jones, A.W., Jones, E. and Williams, E.M., 1973, Vacuum 23, 227.

Kouptsidis, J. and Mathewson, A.G., 1976, DESY 76/49.

Kramers, H.A., 1923, Phil. Mag. 46, 836.

LEP, 1979, 'Design Study of a 22 to 130 GeV e^+e^- Colliding Beam Machine', CERN/ISR-LEP/79-33.

Meredith, W.J. and Massey, J.B., 1968, 'Fundamental Physics of Radiology' (John Wright : Bristol).

Redhead, P.A., Hobson, J.P., and Kornelsen, E.V., 1968, 'The Basis of Ultra-High Vacuum' (Chapman and Hall : London).

Storm, E., Isral, H.I. and Lier, D.W., 1968, Los Alamos Sci. Lab. Report LA-4624.

Storm, E. and Lier, D.W., 1972, Health Physics, 23, 73.

Thompson, D.J., 1975, 'Design Study for a Dedicated Source of Synchrotron Radiation', S.R.C., Daresbury Lab. DL/SRF/RS.

Trickett, B.A., 1978, Vacuum 28, 471.

Unsworth, M.H. and Greening, J.R., 1970, Phys. Med. Biol. 15, 621.

Vaughan-Watkins, R.S. and Williams, E.M., 1978, Vacuum 28, 459, 1980, Proc. 8th Int. Vac. Cong., Cannes, Vol. II, p. 387.

Figure Captions

Fig. 1 Schematic representation of the equipment. G-total pressure gauge; LV - leak valve; X - valve; TM - burbo molecular pump; R.G.A. - residual gas analyser; SP - sputter ion pump; SU - sublimation pump.

Fig. 2 Examples of X-ray spectra recorded at tube voltages of 20, 40 and 80 keV.

Fig. 3 Relative values of efficiency factor k as a function of tube voltage.

Fig. 4 Photon output flux and mean photon energy as a function of tube voltage. Photon flux per second determined at 8 mA tube current.

Fig. 5 Examples of recordings of total and partial pressures accompanying irradiation.

Fig. 6 Pressure pulse heights for desorption of carbon dioxide measured as a function of tube current for two settings, 15 and 40 kV, of the tube voltage. The figures in parenthesis indicate the relative sensitivity.

Fig. 7 The variation of pulse heights, hydrogen partial pressure and total gas pressure, with tube voltage. Tube current set at 8 mA.

Fig. 8 The findings in investigations with extensive photon irradiation. The settings of the X-ray generator corresponding to the stages of irradiation labelled in the diagrams are as follows :
A - 30 kV, 30 mA; B - 60 kV, 25 mA; C - 80 kV, 30 mA;
D - 80 kV, 30 mA; E - 55 kV, 25 mA; F - 30 kV, 50 mA;
G - 30 kV, 50 mA; H - 20 kV. 45 mA;
I - 65 kV, 35 mA; J - 65 kV, 35 mA.

Fig. 9 The photon desorption efficiency as a function of voltage at the X-ray head.

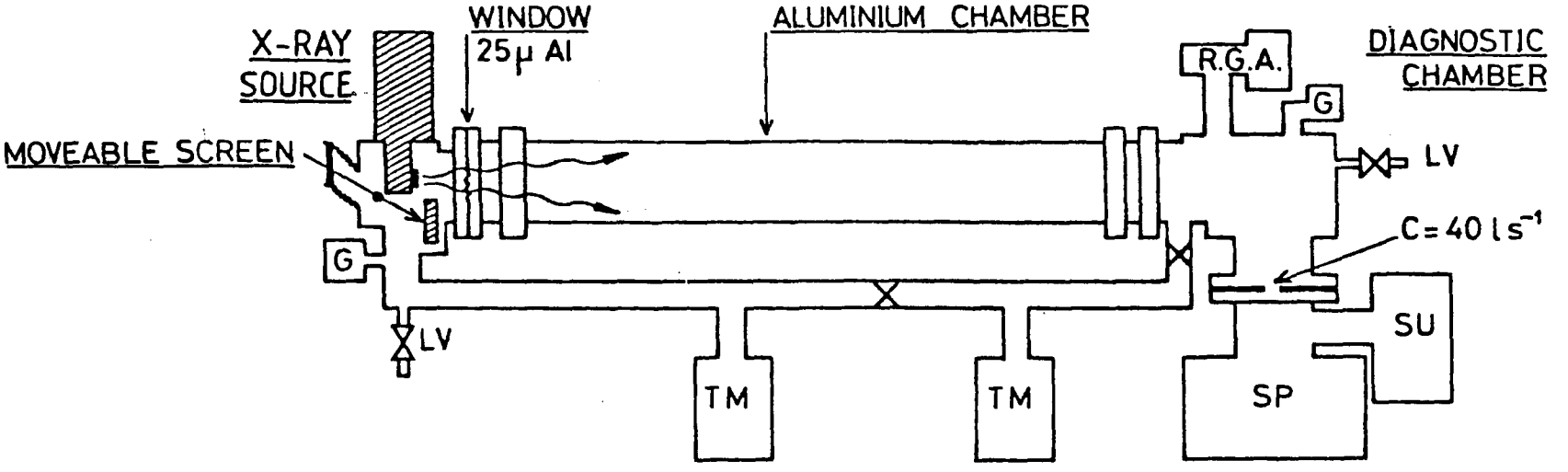
X-RAY SOURCE
WINDOW 25μ Al
ALUMINIUM CHAMBER
R.G.A.
DIAGNOSTIC CHAMBER
MOVEABLE SCREEN
G
LV
C = 40 l s⁻¹
G
LV
TM
TM
SP
SU

FIG.1

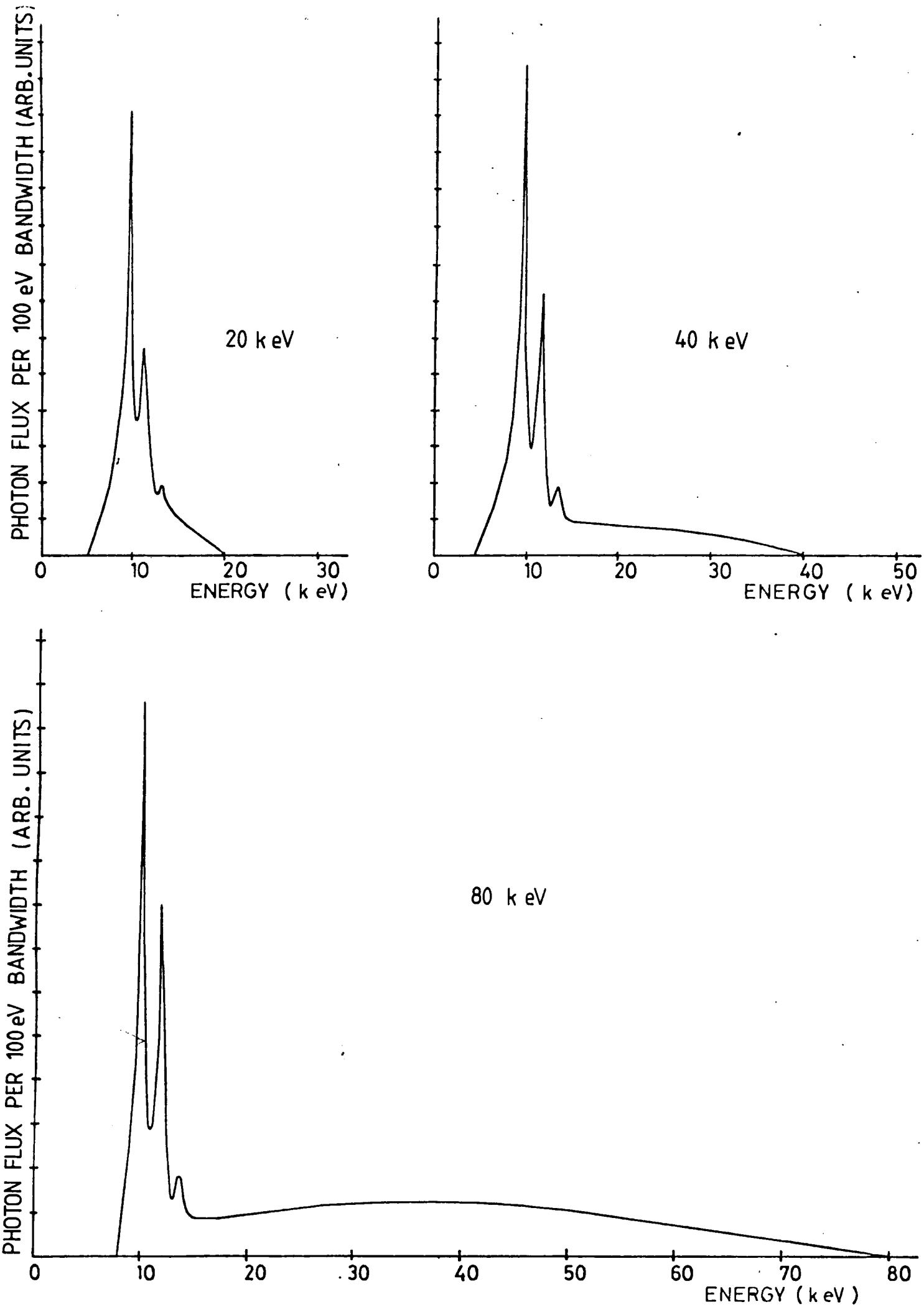
PHOTON FLUX PER 100 eV BANDWIDTH (ARB. UNITS)
20 k eV
0
10
20
30
ENERGY (k eV)
40 k eV
0
10
20
30
40
50
ENERGY (k eV)
PHOTON FLUX PER 100 eV BANDWIDTH (ARB. UNITS)
80 k eV
0
10
20
30
40
50
60
70
80
ENERGY (k eV)

FIG. 2

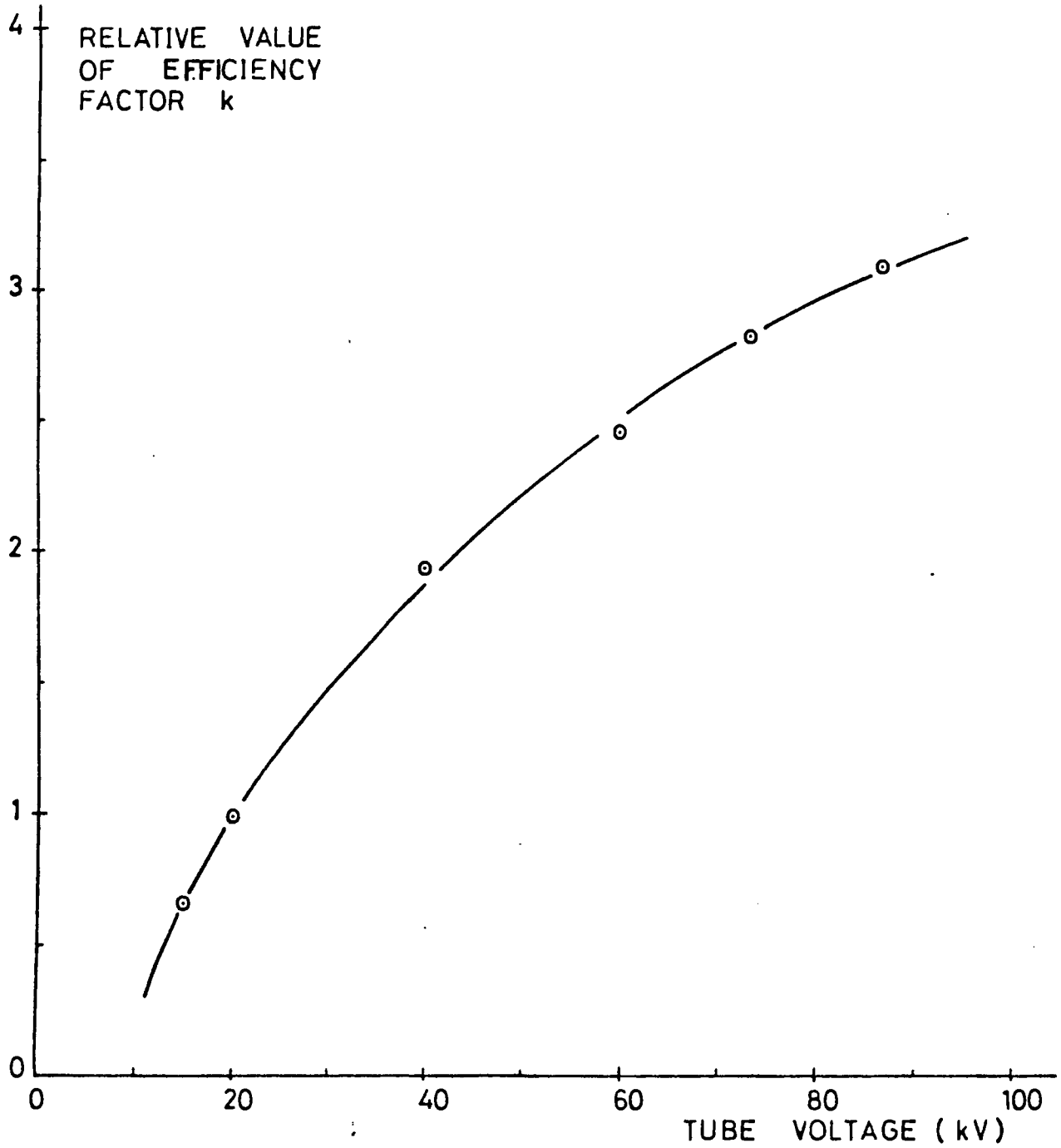
RELATIVE VALUE
OF EFFICIENCY
FACTOR k
4
3
2
1
0
0
20
40
60
80
100
TUBE VOLTAGE (kV)

FIG 3

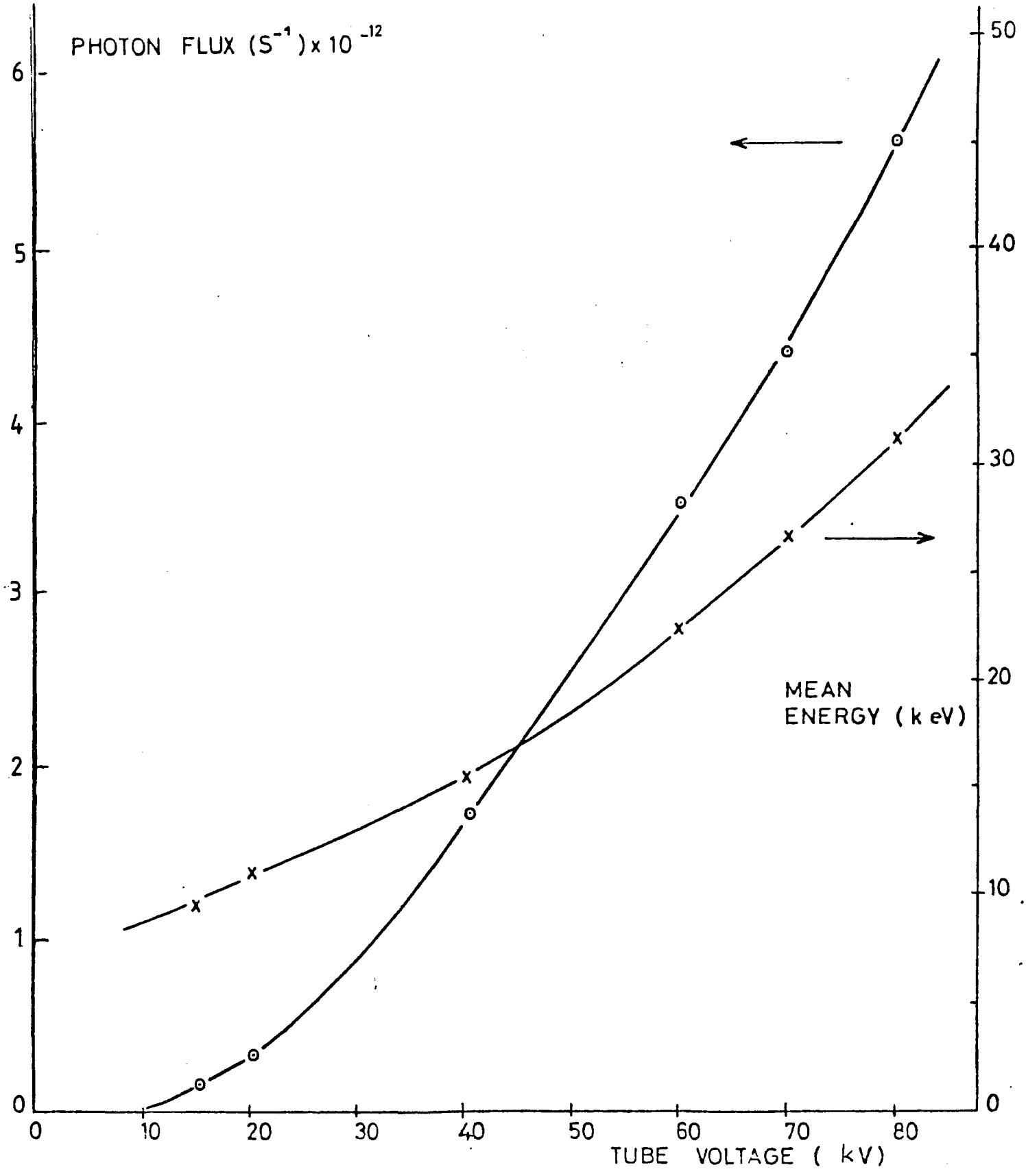
PHOTON FLUX (S^{-1}) x 10^{-12}
6
5
4
3
2
1
0
50
40
30
20
10
0
MEAN
ENERGY (k eV)
0
10
20
30
40
50
60
70
80
TUBE VOLTAGE (kV)

FIG 4

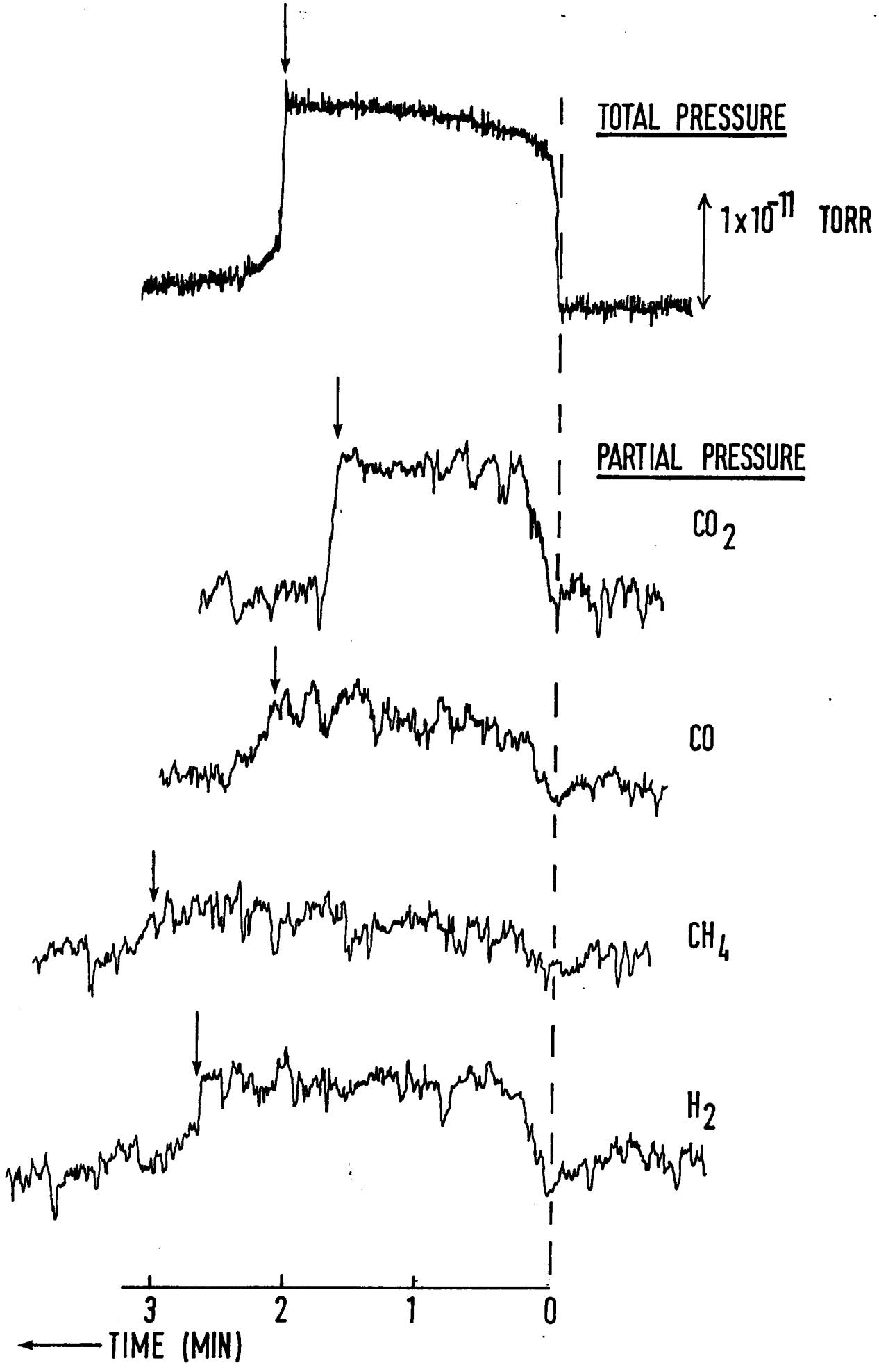
TOTAL PRESSURE
1x10⁻¹¹ TORR
PARTIAL PRESSURE
CO2
CO
CH4
H2
3
2
1
0
TIME (MIN)

FIG. 5.

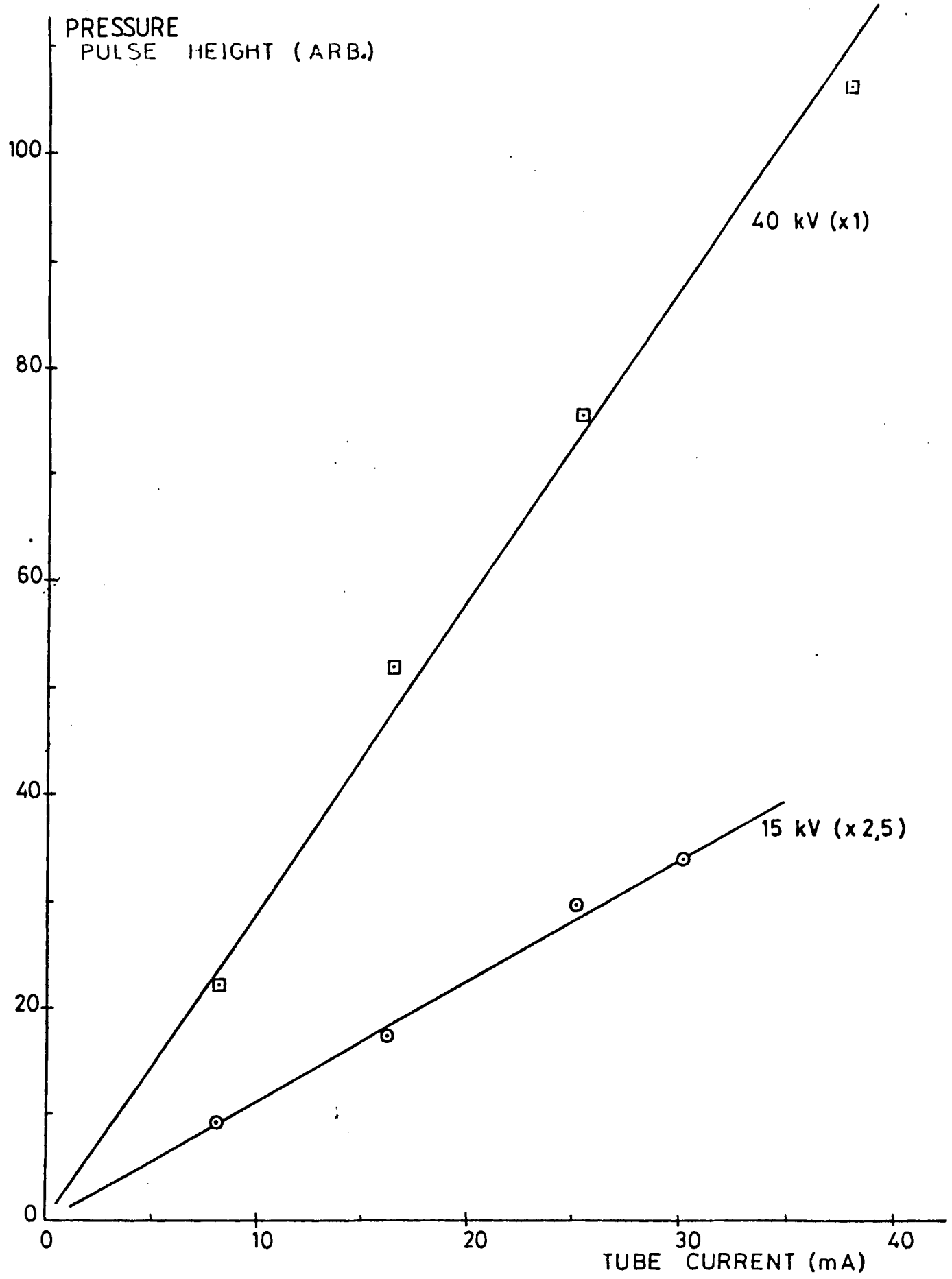
PRESSURE
PULSE HEIGHT (ARB.)
100
80
60
40
20
0
0
10
20
30
40
TUBE CURRENT (mA)
40 kV (x1)
15 kV (x2,5)

FIG. 6

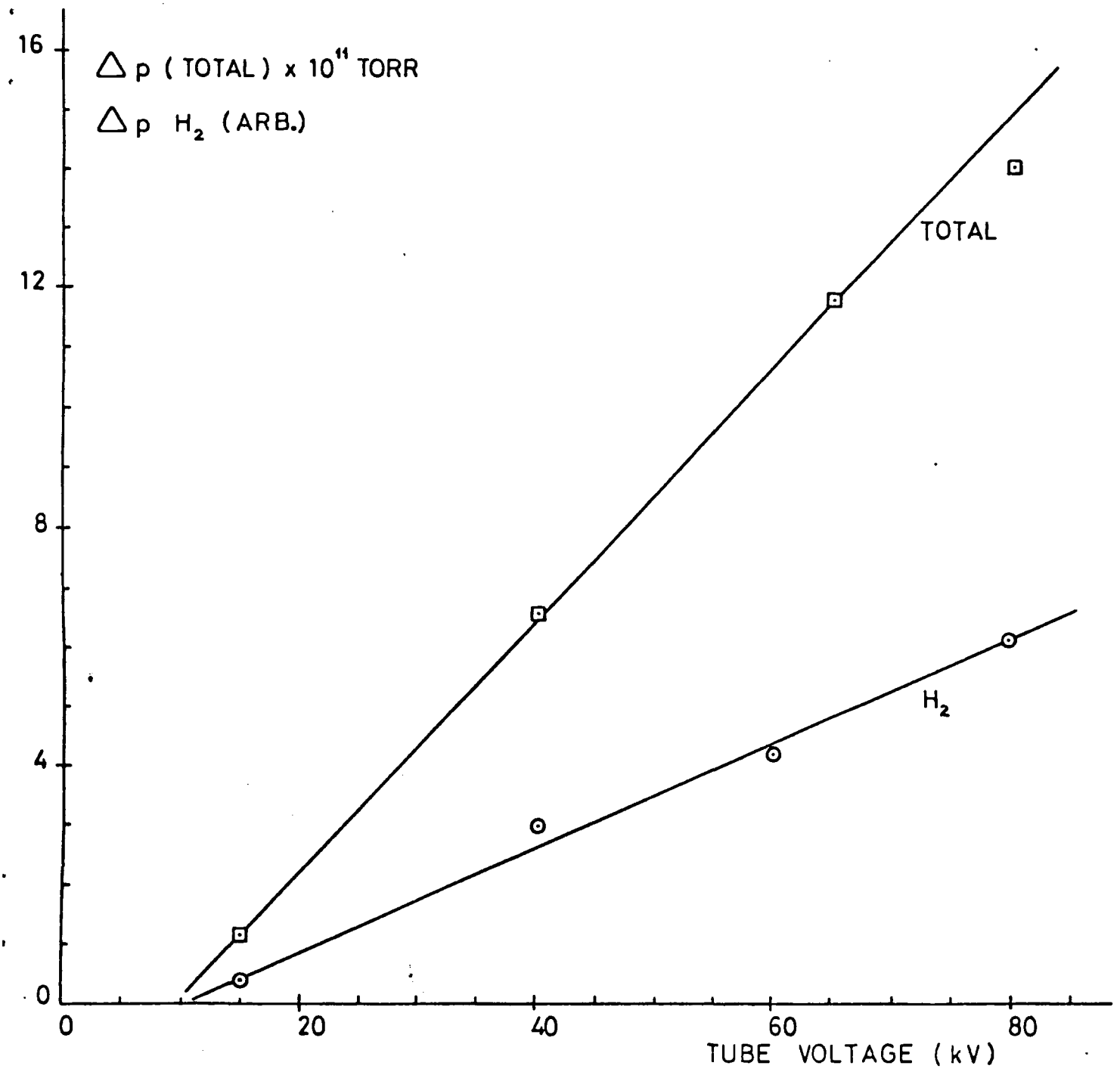
16
12
8
4
0
Δ p (TOTAL) x 10^11 TORR
Δ p H2 (ARB.)
TOTAL
H2
0
20
40
60
80
TUBE VOLTAGE (kV)

FIG.7

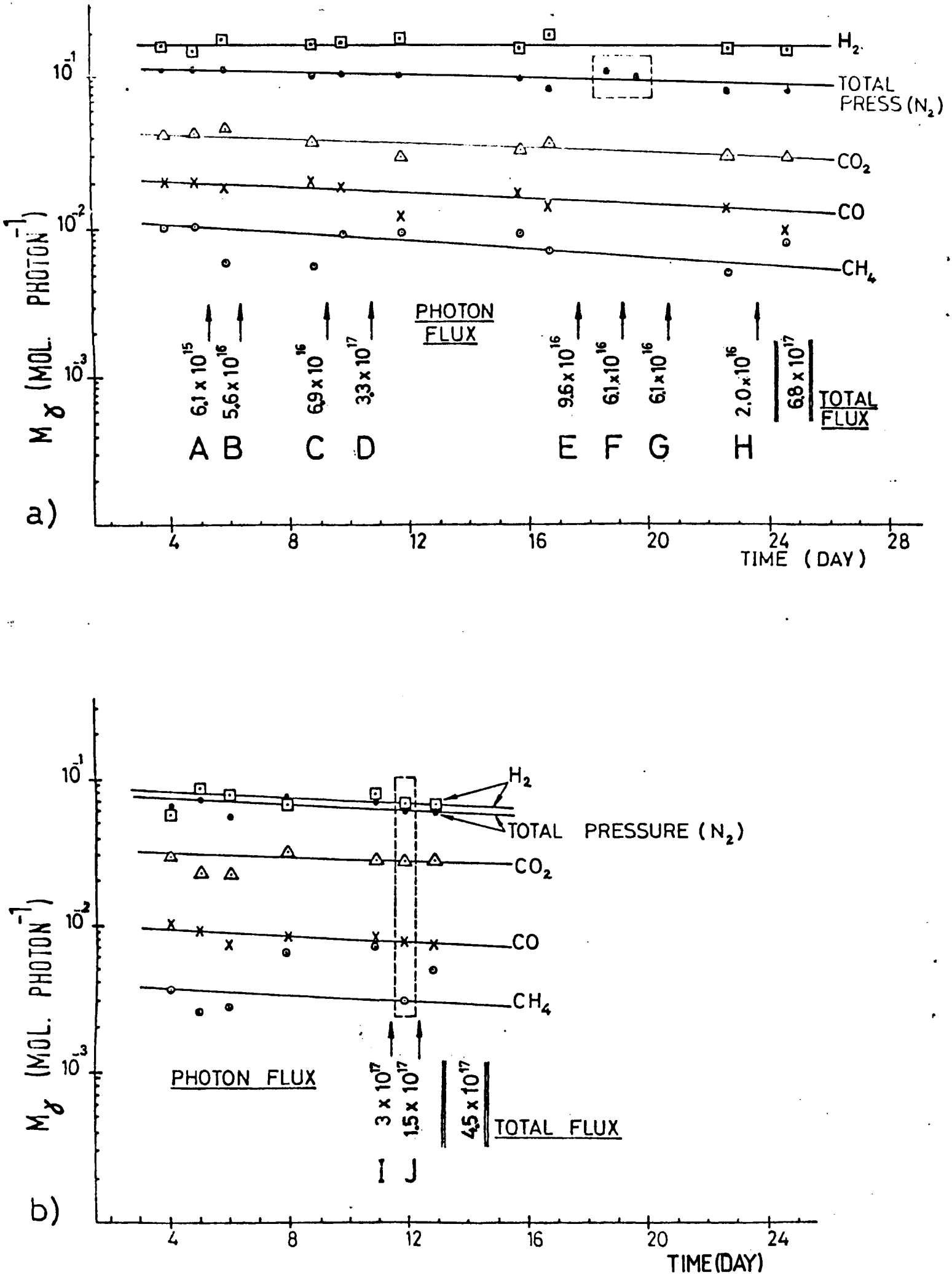
a)
M_γ (MOL. PHOTON^{-1})
10^{-1}
10^{-2}
10^{-3}
H_2
TOTAL PRESS (N_2)
CO_2
CO
CH_4
PHOTON FLUX
6.1 x 10^{15}
5.6 x 10^{16}
6.9 x 10^{16}
3.3 x 10^{17}
9.6 x 10^{16}
6.1 x 10^{16}
6.1 x 10^{16}
2.0 x 10^{16}
6.8 x 10^{17}
TOTAL FLUX
A B C D E F G H
4 8 12 16 20 24 28
TIME (DAY)
b)
M_γ (MOL. PHOTON^{-1})
10^{-1}
10^{-2}
10^{-3}
H_2
TOTAL PRESSURE (N_2)
CO_2
CO
CH_4
PHOTON FLUX
3 x 10^{17}
1.5 x 10^{17}
4.5 x 10^{17}
TOTAL FLUX
I J
4 8 12 16 20 24
TIME (DAY)

FIG 8

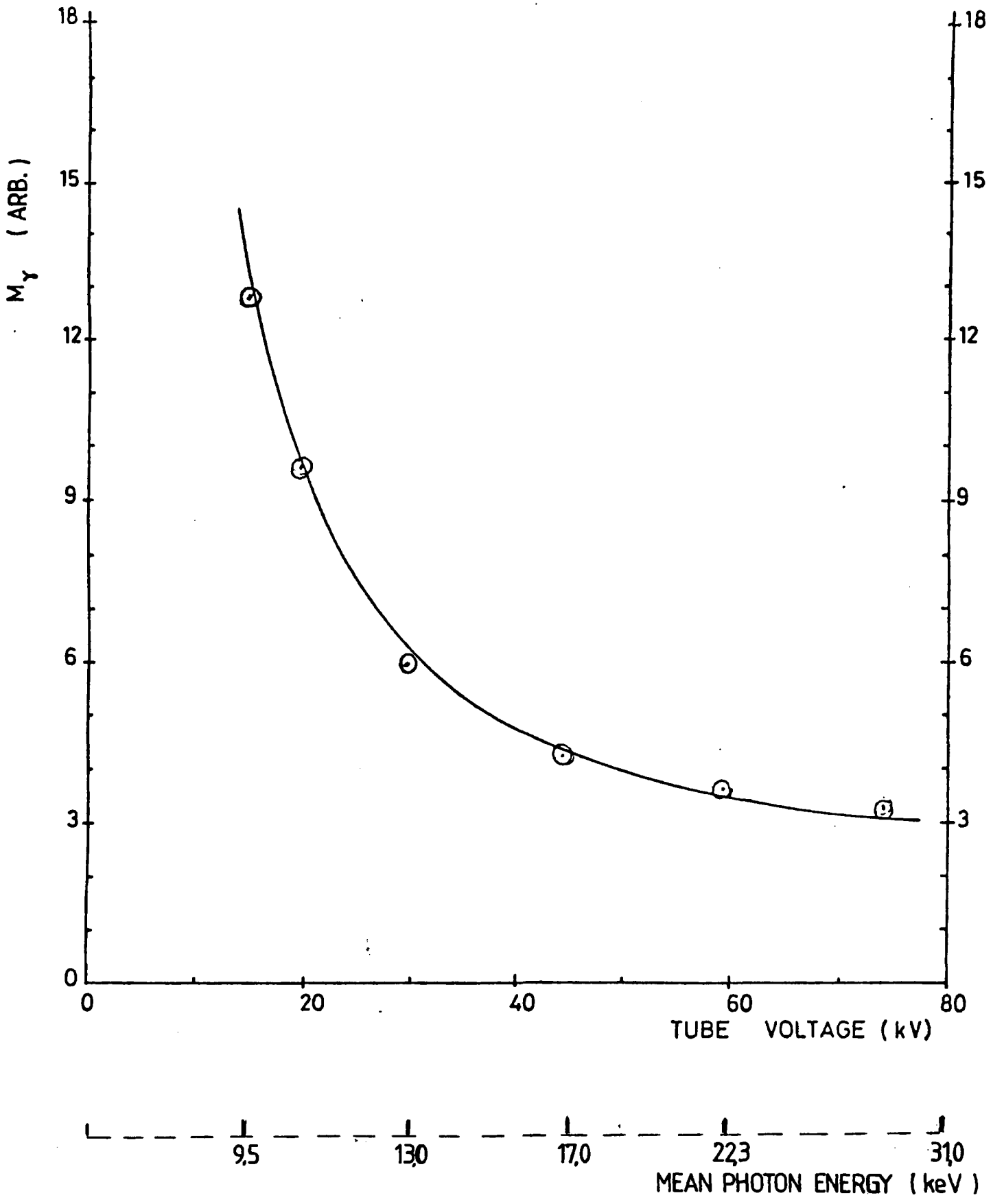
18
15
12
9
6
3
0
M_Y (ARB.)
0
20
40
60
80
TUBE VOLTAGE (kV)
9,5
13,0
17,0
22,3
31,0
MEAN PHOTON ENERGY (keV)

FIG. 9